

LEAK DETECTION IN THE PIERRE AUGER CHERENKOV DETECTORS

A Thesis

Presented for the

Master of Science

Degree

The University of Mississippi

Mark Holcomb

August 2001

To the Graduate Council:

I am submitting herewith a thesis written by Mark Holcomb entitled "Leak Detection In The Pierre Auger Cherenkov Detectors." I have examined the final copy of this thesis for form and content and recommend that it be accepted in partial fulfillment of the requirements for the degree of Master of Science, with a major in Physics.

Lucien Cremaldi, Professor

We have read this thesis
and recommend its acceptance:

Name	Title
------	-------

Name	Title
------	-------

Name	Title
------	-------

Accepted for the Council:

Dean of the Graduate School

ABSTRACT

The purpose of the Pierre Auger project is to study cosmic rays with energies above 10^{18} eV.^{1,2} Two sites with 1600 water Cherenkov detectors spread over an area of 3000 square kilometers are to be constructed. Each Cherenkov detector is filled with 16 KL of water and is expected to operate for 20 years with minimal maintenance. For the Cherenkov detectors to operate correctly the liner must remain nearly full. The focus of this paper is to determine what is an unacceptable defect in a liner, and how to detect the defects before installation.

TABLE OF CONTENTS

Abstract	ii
List Of Figures	iv
List Of Tables	v
CHAPTER	PAGE
I INTRODUCTION TO COSMIC RAYS AND THE PIERRE AUGER PROJECT	1
II CHERENKOV DETECTOR LINER SPECIFICATIONS AND QUALITY CONTROL	6
2.1 Cherenkov Detector	6
2.2 Quality Control	8
III LEAK DETECTION	11
3.1 Light Test	12
3.2 Pressure Test	14
3.2.1 Empirical Parameterization Of Pressure Change Vs. Hole Size	15
3.2.2 Experimental Details	17
3.2.3 Pressure Test Of A Sealed Liner	20
3.2.4 Suggested Pressure Test Procedure	21
3.2.5 Limits Of The Pressure Test	22
3.3 Bubble Test	23
3.4 Rare Gas Test	26
Conclusion	27
Bibliography of List of References	28
Appendix A Calculating Leak Rates For The Pressure Test	32
Appendix B Pressure Test Instrumentation	34
Appendix C Program Listing For Pressure Test Data Acquisition	39

List Of Figures

1	Power Spectrum Of Primary Cosmic Rays	2
2	Schematic Of A Pierre Auger Array	4
3	Depiction Of A Secondary Cosmic Ray Shower	4
4	Depiction Of Pierre Auger Cherenkov Detector	6
5	Picture Of Liner Cross Section	7
6	Predicted And Measure Flow Rates For Unblocked Holes	9
7	Measured Flow Rates For Blocked Holes	9
8	Depiction Of The Testing Apparatus	12
9	Pressure Vs. Time For Two Pressure Tests	16
10	Temperature Vs. Time During A Pressure Test	16
11	Pressure Vs. Time For Various Hole Sizes	19
12	Leak Rate Vs. Hole Size	19
13	Pressure Vs. Time For Permanently Patched GP2	21
14	72-Hour Temperature Record Of Testing Room	23
15	Picture Of Bubble Test Experimental Apparatus	24
16	Predicted And Measured Minimum Pressure To Start A Bubble	25
17	GOW-MAC Output Vs. Time For He Test	26
B.1	Circuit Schematic For Pressure Test Data Acquisition	35
B.2	Linearity And Amplification Test Of Data Acquisition Circuit	37
B.3	2-Hour Pressure Readings At Simulated Constant Pressure	38
B.4	2-Hour Histogram At Simulated Constant Pressure	38

List Of Tables

1	Tank Statistics	6
2	Liner Statistics	7
3	Hole Size Classifications	10
4	Leaks Found With Light Test (GP2)	13
5	Data From Pressure Test Development	18
6	Predicted And Measured Slopes Of A Pressure Test	20
B.1	Linearity And Amplification Test Of Data Acquisition Circuit	36

CHAPTER I

INTRODUCTION TO COSMIC RAYS AND THE PIERRE AUGER PROJECT

Cosmic rays are elemental particles entering the Earth's atmosphere from space. These particles were discovered in 1912 by Victor Hess. Hess observed that an electroscope placed in the balloon discharged more rapidly as it ascended. He attributed the reduced discharge time to radiation entering the atmosphere from space. He was awarded the Nobel Prize in 1936 for his work. Unfortunately, the term "ray", which implies a photon, was used to describe this radiation. Subsequent experiments showed these rays are affected by the Earth's magnetic field, indicating they also include charged particles.

The extraterrestrial cosmic rays, which come from outside the earth, are called primary cosmic rays (PCRs). Secondary cosmic rays (SCRs) are produced as the PCRs collide with atoms in the atmosphere.

Most PCRs have energies between 100 MeV and 10 GeV.³ The flux vs. energy is shown in Figure 1. Up to 10^{15} eV the flux obeys a simple power law where flux is proportional to $E^{-2.7}$. Above 10^{15} eV the flux is proportional to E^{-3} – The number of particles arriving decreases by about a factor of 1000 for every factor of 10 increase in energy.⁴ The highest energy cosmic ray measured to date had more than 3×10^{20} eV.

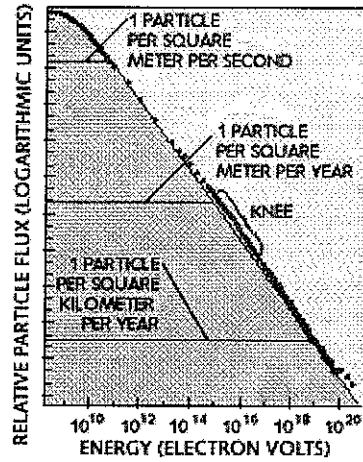


Figure 1¹⁰

Most cosmic rays are thought to get their energy from supernova explosions, which occur approximately once every 50 years in our Galaxy. It is difficult to verify this directly because all charged low energy cosmic rays are deflected by galactic and terrestrial magnetic fields, randomizing their directions.

Cosmic rays can include all of the known elementary particles, complex nuclei, or even unknown entities. About 89% are protons, 10% helium, and about 1% heavier elements.⁵ Electrons make up less than 1% of cosmic rays. High-energy electrons are less abundant due to their emission of synchrotron radiation in route. High energy neutrino and gamma ray interactions in the atmosphere are rare, but the subject of much study.^{6,7,8,9} Secondary cosmic rays are primarily pions, muons, neutrinos, electrons, positrons, and gamma rays. Most particles that reach the surface are muons with an average intensity of about 100 per m^2 per second.¹⁰

In 1938, Pierre Auger discovered extensive air showers of particles produced by the interaction of cosmic ray particles with the earth's atmosphere.¹¹ The Pierre Auger Project is named in his honor. Auger showed that detectors placed near each other on the

ground recorded simultaneous events. This led to the idea of the “shower” of secondary particles created by a single primary particle. As described later, observation of this “shower” is the primary method of studying PCR's with very low flux.

In 1991 the "Fly's Eye" detector in Utah observed an incoming particle from space with an energy over 3×10^{20} eV, six times higher than was thought possible.⁹ Two years later the Akeno Observatory in Japan recorded a similar event. These two cases have motivated the international community to build a detector large enough to detect these high-energy cosmic rays in greater number.

Above the energy of 10^{18} eV the flux is approximately one particle per week per square kilometer. Above the energy of 10^{20} eV, only one particle falls on a square kilometer in a century.¹⁰ To study these particles in sufficient number a very large detector is needed, thus the origin of the Pierre Auger Project.^{12,13,14,15,16}

The Pierre Auger Project will be composed of two detectors, one in the Southern Hemisphere and one in the Northern Hemisphere. The detector in the Southern Hemisphere is now being constructed in Mendoza, Argentina. The Northern Hemisphere detector will be located in Utah.

Extensive air showers are produced when these high-energy cosmic rays enter the atmosphere. The Pierre Auger project uses two kinds of detectors to study these showers. The first method consists of 1600 water Cherenkov^{17,18} detectors spread over an area of 3000 square kilometers. The second method uses optical detectors that record atmospheric fluorescence light.¹⁹ The Cherenkov detectors allow measurement of the spatial and temporal structure of the shower on the surface, and the fluorescence detectors measure the longitudinal aspect in the atmosphere. The fluorescence detectors only work

effectively on clear nights. Therefore, only about 10% of the showers observed by Auger will be seen by both detectors.¹⁹

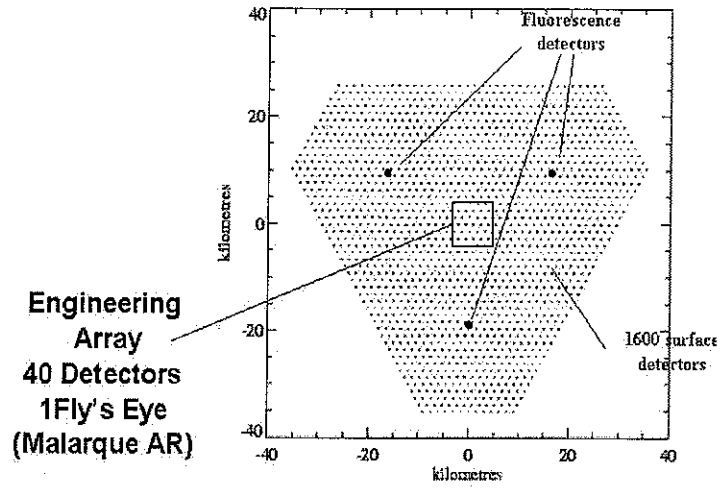


Figure 2

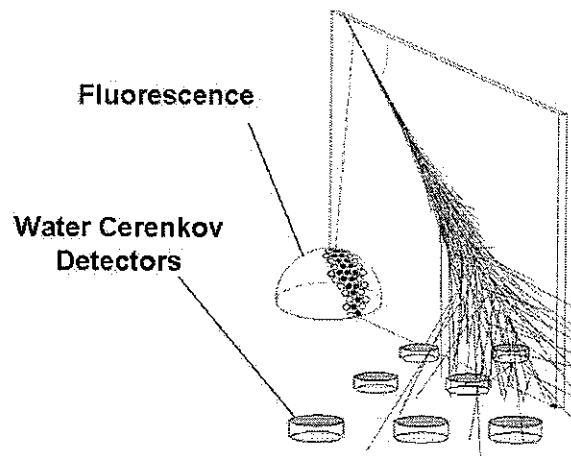


Figure 3

The extremely high energy of these cosmic rays aids their study. Given the large Lorentz factor for particles at these high energies, their trajectories are not randomized by galactic magnetic fields. Assuming a magnetic field of a few micro-Gauss inside the galaxy, the particles should point to within a few degrees of their source.²⁰

A maximum distance to the source of these particles of 100 Mpc was predicted by Greisen-Zatsepin- Kuz'min, called the GZK cutoff.^{4,21} Essentially the GZK cutoff takes in to account the strong propagation losses that affect the particles in their journey from their source to Earth as they interact with the microwave background.

There is no well-established mechanism that can accelerate particles above 10^{20} eV. The mystery is deepens when the 100 Mpc distance is also considered -- Whatever this unknown source is, it must be within our local supercluster of galaxies. While there is no well-established acceleration mechanism, there is no shortage of theories.^{22,23} Possibilities include Topological Defects and decays of ultra-heavy particles, and neutrinos of exotic origins.^{24,25,26,27}

CHAPTER II
CHERENKOV DETECTOR LINER SPECIFICATIONS AND QUALITY
CONTROL

2.1 Cherenkov Detector

The ground array consists of a set of water Cherenkov detectors. Each tank of the Auger array will be filled with 16 KL of water. The water is hermetically sealed in a Tyvek laminated liner that is placed inside the tank. The configuration and instrumentation of the detector is shown in Figure 4.

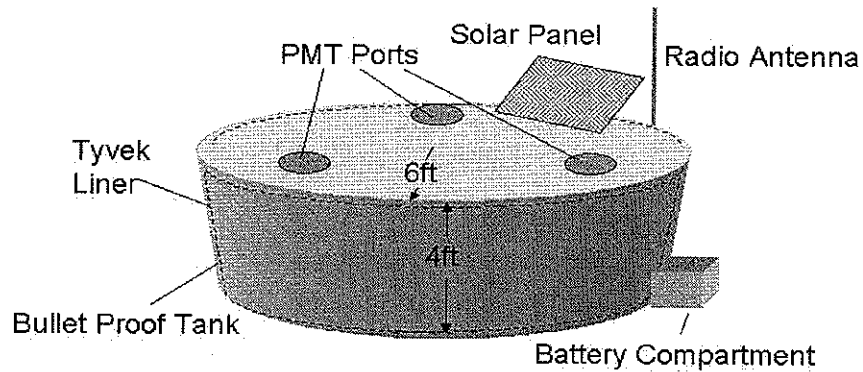


Figure 4

The tank and liner statistics are shown in Tables 1 and 2. A cross section of the four layers of the liner are shown in Figure 5.

Tank Statistics

Height	Radius	Total Surface Area	Volume
4 ft	6ft	377 ft^2	452 ft^3

Table 1

Liner Statistics

Material	Thickness
Tyvek	5.6 mils
LLDPE	1.1 mils
Black LLDPE	4.5 mils
m-LLDPE	1.0 mils

Table 2

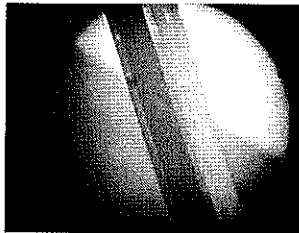


Figure 5

Tyvek was selected because of its good UV reflectivity characteristics. The outer layers of LLDPE prevent outside light from entering the detector – Only Cherenkov light should be seen by the photomultiplier tubes (PMTs). On top of the liner are three acrylic domes where the three PMT's are attached. PMTs observe the Cherenkov light created in water by the charged particles. The Cherenkov light signal is measured by the number of photoelectrons generated at the tube cathode and the total charge collected at the tube anode.

Electronic signals from the PMTs are fed into the front-end electronics. The triggering electronics determine what is a “good” event by taking into account the energies and timings of the signal. These signals are recorded and transmitted to a central station by the communications hardware.

The detector is equipped with a solar powered battery system. A GPS antenna provides accurate timing information to 10 ns that allows synchronization with events recorded in other detectors.

2.2 Quality Control

One of Auger's technical challenges is to produce a liner which will retain 90% of the initial fill water over the expected 20-year life of the experiment. Therefore, a leak rate of less than 60L/Year is required.²⁸

It is the focus of our investigations to determine methods by which liners can be inspected insuring that small holes will be detected. Leaks may occur through a diffusion characterized by a Moisture Vapor Transfer Rate (MVTR) or directly through holes and ruptures.

MVTR describes the amount of water diffusing through the laminate from wet to dry sides. The MVTR of polyethylene (PDPE) is approximately 0.1g/24h/100 in² per mil (0.001 inch) of LDPE. It is estimated the MVTR will be less than 0.014g/24hr/100 in². Using a surface area of approximately 380 ft², this corresponds to less than 10 ml per day. Therefore, MVTR will account for only a few percent of the allowable leak rate.²⁸

Primary leaks will occur through holes in the liner. Investigations were conducted to determine the flow rates of water under the pressures of interest (0-1.2 m H₂O) through unblocked holes as well as holes pressed against a wall. The apparatus used were simple containers with laminate attached to one end to which holes of various sizes were added. We predicted the leak rates with the Bernoulli Equation. Neglecting drag, $\Delta P = (1/2)\rho v^2$. The volume flow rate (Q) through the hole is given by $Q=vA_{\text{eff}}$. For blocked holes A_{eff} is calculated as shown below.²⁸

$$A_{eff} = \left(\frac{1}{A_{open}} + \frac{1}{A_{closed}} \right)^{-1} \quad (2.2)$$

Where $A_{open} = \pi R^2$, $A_{closed} = 2\pi R\delta$, and $\delta =$ gap spacing between laminate and wall. Note that if $R \ll \delta$, A_{eff} approaches A_{open} .

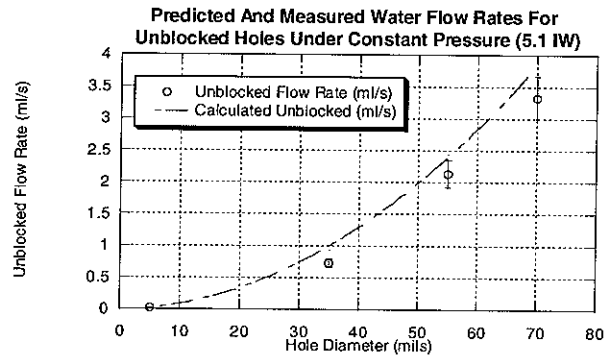


Figure 6

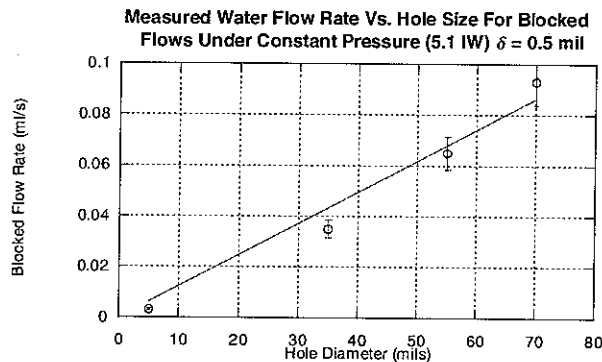


Figure 7

Some measurements of the leak rates of blocked and unblocked holes versus hole size are shown in Figures 6 and 7. The experiments show that the leak rate of an unblocked hole is very close to that predicted by Bernoulli's equation.

The flow of blocked holes was difficult to calculate due to the unknown δ . The measured blocked flow rates at a given pressure and hole size varied significantly. One possible reason for this is a slightly different δ when the experiment was repeated. The

hole diameters used ranged from 5 mil to 95mil. The δ was estimated to be 0.5 mil. Note $R_{\text{hole}} \gg \delta$. While difficult to closely repeat results, it is clear from the data that the flow through an unblocked hole is proportional to R^2 , and the flow through a blocked hole is proportional to R . This qualitatively validates the expression for A_{eff} .

Assuming a worst-case pressure of 1.22 m of H_2O and a δ of 0.5 mil, Table 3 lists what we define as small, medium, and large holes.

Hole Size Classifications

Category	Diameter (D) of Circular Hole (mils)	Calculated Leak Rate (Q) (L/Year)
Small Holes	$D < 1$ mil	$Q < 60$
Medium Holes	$1 \text{ mil} < D < 80$ mil	$60 < Q < 5000$
Large Holes	$D > 80$ mil	$Q > 5000$

Table 3

The remainder of the paper deals primarily with hole detection by various means.

CHAPTER III

LEAK DETECTION

Four methods of leak detection were considered:

1. Light Test
2. Pressure Test
3. Rare Gas Test
4. Bubble Test

Two liners were inspected in developing the tests discussed in the paper. The first liner (GP1) was a prototype that had been extensively handled. The second liner (GP2) was new, recently fabricated in China. GP2 was slightly damaged during our tests though. Upon over pressurizing a seam came apart, the region affected was approximately 9 ft long along the bottom seam. This region was patched with duct tape, and clamped with curved wooden strips about the seam. In addition, two other large holes were created by a light bulb in another test, and two gashes were caused by an instrument falling off a table and striking the liner. These were approximately 2 cm long and 2 mm wide. All were temporarily patched with duct tape.

Figure 8 illustrates the testing lab which was outfitted with a shop vac/air compressor system to inflate the liner and pressure/temperature monitoring transducers. He and CO₂ bottles were attached to the gas system for leak testing. The windows of the room were light-sealed for testing under darkness during the day.

Testing Apparatus

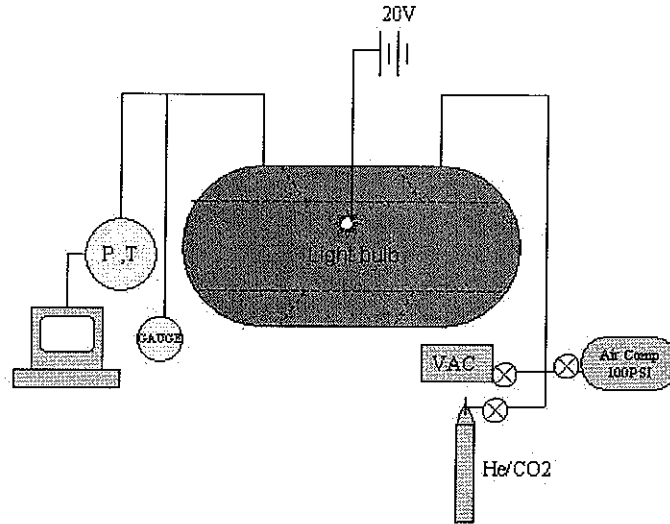


Figure 8

3.1 Light Test

The Auger liner is opaque and designed to trap Cherenkov light inside until reflected to a PMT or absorbed. By illuminating the interior of the liner with a bulb we were able to devise an effective test.

A light bulb was lowered into the liner through one of the three fill ports. A low wattage light source was used so as not to damage the liner. We used two 20-watt (at 12V) automotive bulbs connected in series. The power cord was lowered through a small hole drilled in to one of the fill caps. A VARIAC set at 20V RMS was used as the power source. Two advantages of this method are the bulbs are not hot enough to do damage to the liner, and the supply voltage is much safer than line voltage.

After our eyes were sufficiently dark-adapted we could easily see small holes in the liner. A close inspection revealed a number of apparent leaks. After inspection many

holes in both GP1 and GP2 were found using this technique. At this point all light leaks did not appear to be through-holes but translucent areas. The following table summarizes the holes found in GP2 using the Light Test.

Leaks Found With Light Test (GP2)

Location On Liner	Number Found	Size	Number Through Liner
Seams	14	Width < 1mm Length 1-10 mm	3
Body	0	N/A	N/A
Optical Kit	2	Width < 1mm Length 2-3mm	2

Table 4

Many holes found had diameters less than 10 mil. In order to determine the smallest hole that is detectable with the light test a 5 mil diameter puncture was made in a piece of the laminate. The laminate was attached over one of the fill holes and secured with tape. With the bulb not in the line of sight, the 5-mil hole was easily seen. A polarizer was placed between the hole and observer, and the hole was still readily detectable. Based on this experiment, it is estimated that with the light source used, a hole with diameter approximately 3.5-mil, or 0.006 mm^2 can be readily detected.

Room darkness and the observer can significantly affect the detectable hole size. It also takes two or three minutes for the observer's eyes to adapt to the dark. Of course, adding more bulbs would decrease the size of a detectable hole.

As previously mentioned many of the holes not on a seam appear to be punctures. Light through these holes may be easily visible at one angle, and not visible at another.

So when conducting the light test it is important to look at each region of the liner from different angles.

The light test showed many apparent holes near the seams in both liners that were inspected. Some of these were areas where the outside of the liner had apparently melted during construction of the seam. Both Tyvek and the bonding plastic used to make the seam are somewhat translucent, and appear to be a hole when using the light test. Visual inspection with a magnifier and bubble test suggested that many of the defects do not go entirely through the liner. Even though a defect does not go completely through the liner, a translucent area does represent a weak spot. Also, the MVTR in this area could be significantly higher, and it could allow external light to enter one of the PMTs.

We believe the light test is a very effective method of quickly finding small holes in the liner.

3.2 Pressure Test

The pressure test can be used to find medium to large holes. The liner is inflated and the pressure is monitored over time. From the change in pressure the cumulative hole size of the liner can be determined.

A Craftsman 5.5 HP Wet/Dry Vac (Blower), and A 5 HP Campbell Hausfeld air compressor were used to inflate the liner. The hose from the blower was inserted directly in one of the fill holes. Great care should be taken when using the blower to inflate the liner. Once the pressure in the liner starts to rise above atmospheric, it only takes a few seconds to rise to several IW (Inches of Water). On GP2 a seam came apart at about 4 IW, and others reported the same thing at about 2.5 IW. It is recommended that the

maximum inflation pressure used be under 2.1 IW for an unsupported liner. As shown later, these low pressures still allow a sensitive leak test.

3.2.1 Empirical Parameterization of Pressure Change Vs. Hole Size

Some attempts were made to determine the leak rate of liners under changing pressure and volume conditions (see Appendix A). These were abandoned and a simple parameterization assuming constant volume and temperature conditions was used.

The parameterization was performed by introducing small holes of known sizes in a patch. The liner was inflated and the pressure and deflation rate was monitored. Based on the rate of deflation for each known hole size, we could then estimate the size of an unknown hole.

In order to determine the effective area of holes in the liner, we assume the liner remained at a constant volume between 1 and 1.5 IW. Between these pressures there is no measurable change in height or circumference. The constant volume assumption is buttressed by observing the rate at which the air compressor pressurizes the liner – Once the pressure reaches a few tenths IW, the pressure quickly and uniformly rises to 2.0 IW.

A constant temperature is also assumed during the measurement time. The data for the two graphs in Figure 9 was taken immediately after the liner was inflated. Note the exponential decrease in pressure in the first 500s in both graphs. Both curves exhibit this behavior even though the second begins at a pressure where the first has leveled off.

Pressure Vs. Time For Two Pressure Tests

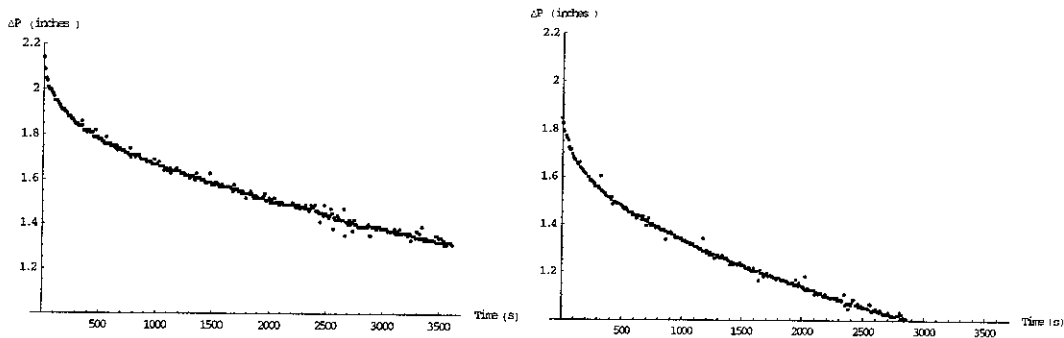


Figure 9

This initial rapid decrease in pressure is thought to be caused by the slightly warmer air used in filling the liner. As the air in the liner comes into equilibrium with the air in the room, dP/dt becomes constant. We tested the idea by monitoring the inside and outside temperature as we filled. The results are shown in Figure 10. A $\sim 0.2^{\circ}\text{C}$ temperature shift was observed.

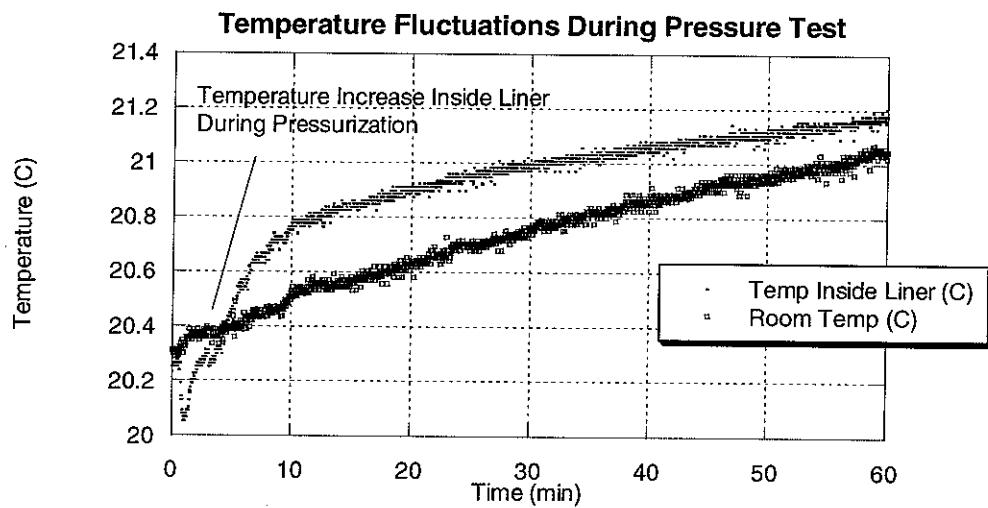


Figure 10

We calculate the pressure increase due to this 0.2°C temperature increase inside the liner for reference. From the Ideal Gas Law:

$$\frac{P_i}{P_f} \propto \frac{T_i}{T_f} \Rightarrow P_f = \frac{P_i T_f}{T_i} = \frac{(1.0130 \times 10^5 \text{ Pa})(300.2 \text{ K})}{300 \text{ K}} = 1.0137 \times 10^5 \text{ Pa} \quad (3.1)$$

$$\Delta P = P_f - P_i = 1.0137 \times 10^5 \text{ Pa} - 1.0130 \times 10^5 \text{ Pa} = 70 \text{ Pa} = 0.27 \text{ IW} \quad (3.2)$$

The nearly .3 IW pressure drop due to a 0.2°C temperature increase can easily account for the initial exponential drop in pressure.

3.2.2 Experimental Details

To initiate the test the blower was used to inflate the liner to 1 IW, and the air compressor and tank were used to slowly raise the pressure to 2.1 IW. A ¼ inch tube from the compressor was connected to one of the fill caps. This allowed the airflow to be simply turned off when necessary. The pressure was then monitored for approximately one hour or longer.

Five inflation tests were performed on this temporarily patched liner (GP2), the first with no added holes, followed by tests with increasing hole size from 3.14 mm² to 63.28 mm². The holes were added by making punctures in a piece of duct tape placed on one of the large holes before they were patched. The total hole size for each test was the added hole size plus the unknown hole size of the liner (x).

Data From Pressure Test Development

Added Hole Diameter	Added Hole Area	dP/dt Of Best Fit Line
mm	mm ²	Inches/Second
2.00	3.14+x	$.00054 \pm 1.74 \times 10^{-6}$
2.82	6.28+x	$.00080 \pm 5.77 \times 10^{-6}$
6.00	28.3+x	$.00233 \pm 7.65 \times 10^{-5}$
9.00	63.6+x	$.00528 \pm 2.4 \times 10^{-4}$

Table 5

As expected, the dP/dt is directly proportional to hole size. Each curve can be represented by a straight line with a very small uncertainty. After fitting the above data, the unknown hole size could be determined from the intercept. The unknown hole size was determined to be 4.0 mm² (10%). A pressure test was performed on the sealed liner before and after the above data was taken. The results were consistent, even though we suspected the temporary patches were leaking. The two tests were in good agreement. The data from all pressure tests are shown in Figure 11. Note the effective unknown hole size of the temporarily patched liner that was determined from the intercept is added to the added hole sizes from Table 5.

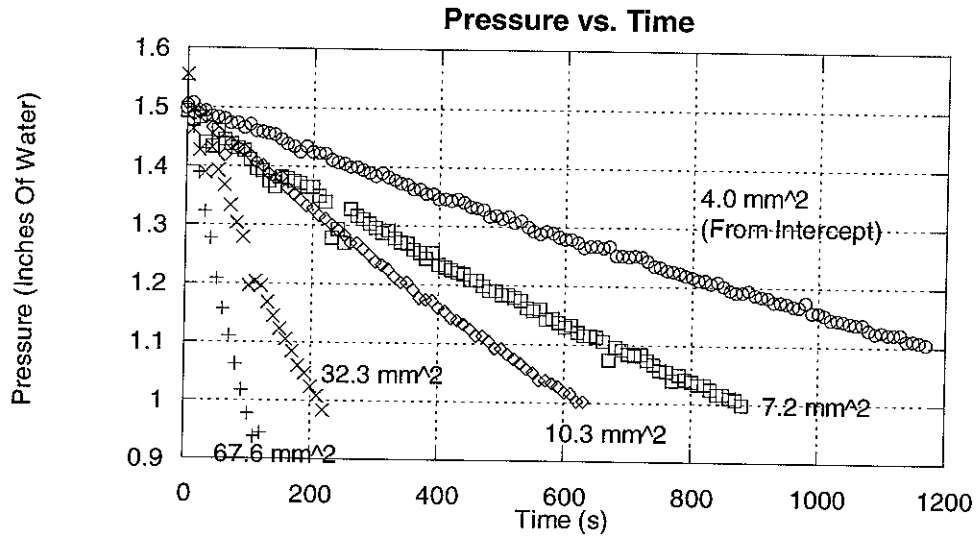


Figure 11

The slope, dP/dt , of each pressure test was determined and plotted in Figure 11. The largest uncertainty in the measurement is the added hole size. A 10% error in diameter for the two smaller holes, and a 5% error in the diameter of the two larger holes was assumed. These propagated errors are displayed in the Fig. 12.

Leak Rate Vs Hole Size

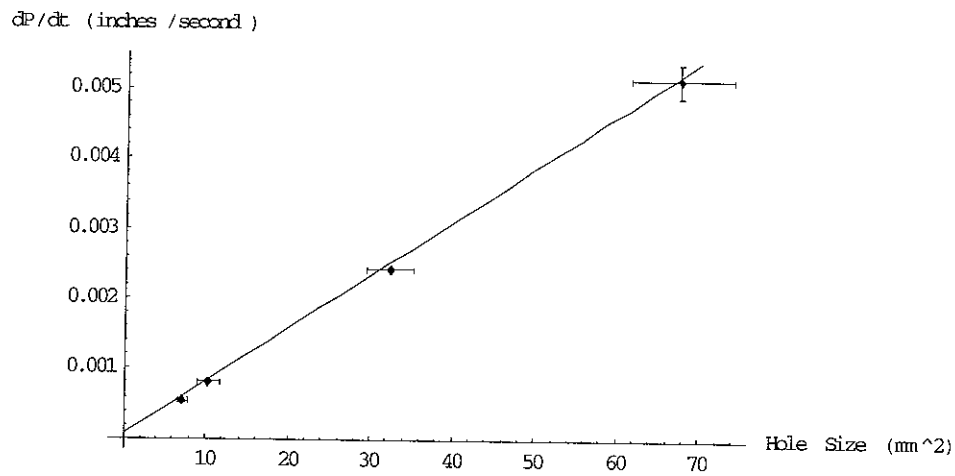


Figure 12

The best fit for this graph is $\frac{dP}{dt} = 0.0000761a$. Where $\frac{dP}{dt}$ is in inches/sec and a (hole size) is in square mm. Taking into account the errors in slope and hole size, the final relation is

$$a = \frac{dP}{dt} 1.31 \times 10^4 \quad \pm 10\% \quad (3.3)$$

Table 6 shows the added hole sizes, measured slopes, and predicted hole sizes based on the empirical formula. The correspondence is good.

Added Hole Size mm ²	Slope Of Best Fit Line Inches/Second	Predicted Hole Size From Slope and Empirical Formula
0.00	.00	0.00
7.14	.00054	7.10
10.28	.00080	10.51
32.3	.00233	30.62
67.6	.00528	69.38

Table 6

After the permanent patches were made, the experiment was repeated by adding three different hole sizes to one of the fill caps and the results were consistent with the original test.

3.2.3 Pressure Test Of A Sealed Liner – GP2

After the parameterization work GP2 was permanently patched using a section of the laminate and RTV. Our pressure test was run and results are shown in Fig. 12. A linear fit gave a dP/dt for the patched liner of 1.49×10^{-6} IW/s. This corresponds to a hole

size of 0.015 mm^2 based on Eq. 3.3. It was obvious from the data that that the permanent patches were much more effective than the temporary.

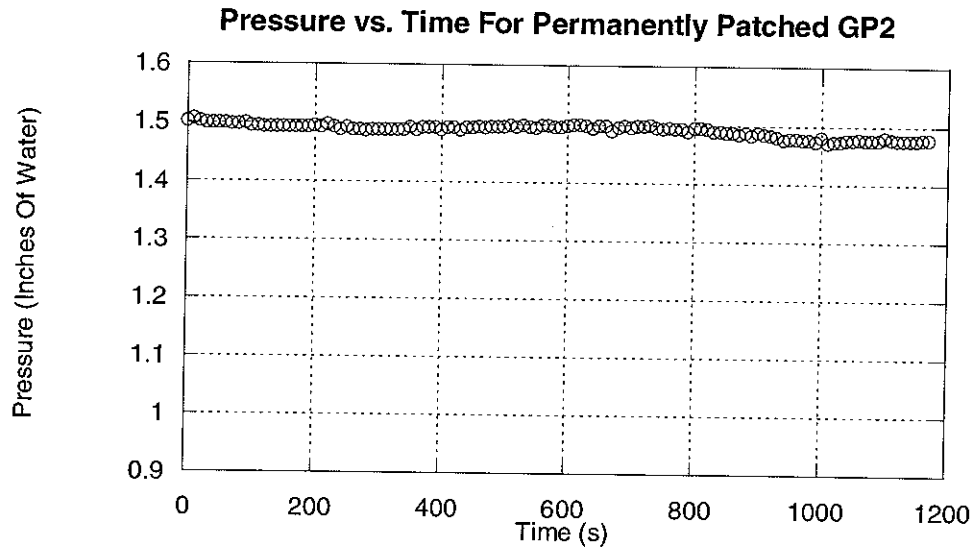


Figure 13

3.2.4 Suggested Pressure Test Procedure

Since it has been established that dP/dt is nearly constant, the data acquisition may not be needed to perform the test. An alternative would be to record the beginning and ending pressures over some length of time. Since any hole size detected by the pressure test would be unacceptably large, this may be the preferred method.

The following suggests a procedure for a simple pressure test:

1. Pressurize liner to 2.1 IW.
2. Wait 10 minutes for temperature to stabilize.
3. If pressure has fallen below 1.5 IW in this time, there is an unknown size but very large hole in the liner.

4. Lower pressure to 1.5 IW or less. Take pressure readings for one hour or until pressure falls below 1.0 IW. Determine dP/dt and use $a = 1.31 \times 10^4 \frac{dP}{dt}$ where a is in mm^2 and P is in IW. Only use data between 1.5 IW and 1.0 IW.

3.2.5 Limits Of The Pressure Test

Various factors can affect the sensitivity of the pressure test. Variation of outside temperature, atmospheric pressure, and drift in the instruments used can all cause errors.

The GP2 patched liner had a leak rate of 1.49×10^{-6} IW/s. Checking with Table 5 this corresponds to a typical measurement error and represents the limit of the accuracy of the pressure test.

According to Equation 3.3 this translates into a hole size of 0.015 mm^2 . This is two orders of magnitude smaller in size than what was used in developing the empirical formula. Over a one hour pressure test, that slope corresponds to a ΔP of 0.005 IW. Recall a 0.2°C change in temperature will cause a change in pressure of 0.27 IW. Fig. 14 shows the temperatures inside and outside an inflated liner for 72-hours. Note the time delay between the temperature fluctuations. A Barometer was used to monitor atmospheric pressure over a two-week period. During stable weather conditions atmospheric pressure can easily change by 0.1 IW.

So, a slope as small as given by the pressure test on patched GP2 is essentially meaningless – the liner could have a hole significantly larger than the empirical formula suggests, or no hole at all. Unless environmental controls and monitors were used, the reasonable lower limit of detectable hole size is thought to be 3 mm^2 .

After the liner is inflated to 2.1IW, some small holes, even smaller than can be detected by the pressure test, have been heard whistling. The shape of the hole is probably as much a factor as size. Walking around the liner and listening during the first part of an inflation test is another quick way to check for leaks. This has the additional advantage of actually locating the hole, which the pressure test lacks.

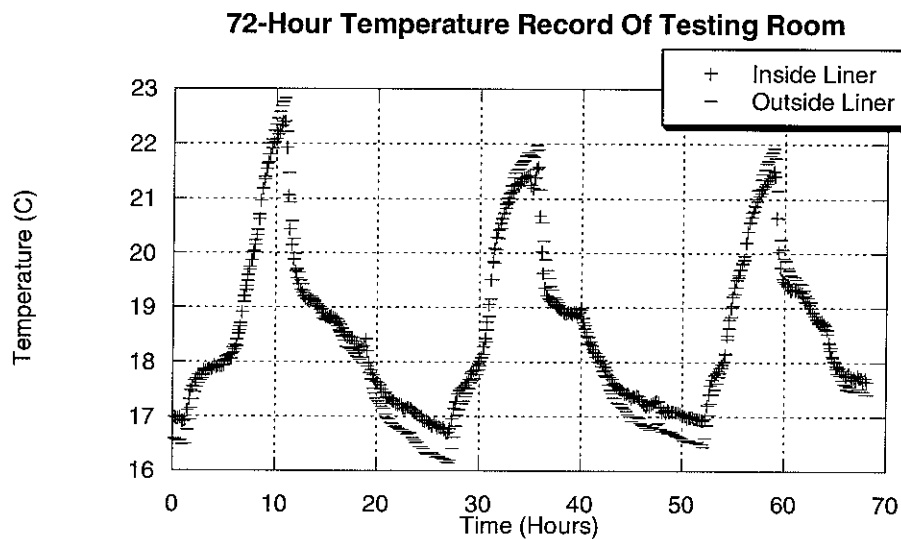


Figure 14

3.3 Bubble Test

The bubble test is performed by inflating the liner with air, then spreading soap water over a small area. Experiments were conducted using a piece of the laminate connected to one end of a PVC pipe as shown in Figure 14. Holes were added to the laminate and the minimum pressure to start a bubble for a given hole size was studied. Several soap water mixtures were used, the most effective was “Mr. Bubbles” manufactured by TOOTSietoY.

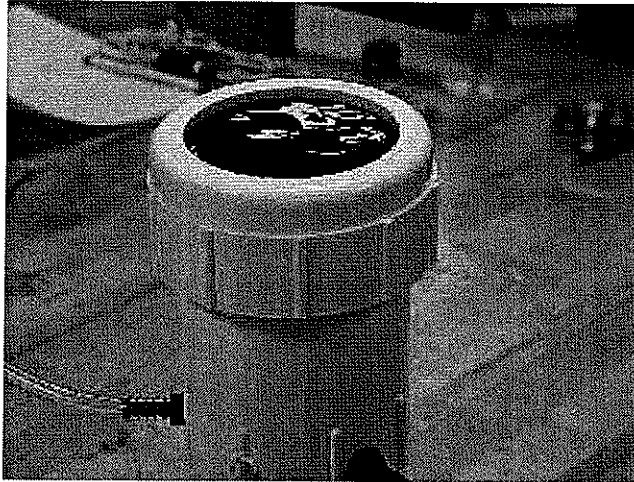


Figure 15

Assuming a circular hole, the length the surface tension acts over is the circumference of the hole. The force due to ΔP is PA , where A is the area of the hole. Taking into account a bubble has two sides, a bubble can begin to form when $P\pi R^2 > \gamma 4\pi R$, where γ is the surface tension and R is the radius of the hole. An approximate value of γ for common soap water is 0.025 N/m. Using 0.020 N/m for γ , Equation 3.4 gives the minimum pressure to start a bubble for a given diameter.

$$P_{\min} = \left(\frac{25.3}{D} \right) \text{ Where diameter } D \text{ is in mils, and } P_{\min} \text{ is in IW.} \quad (3.4)$$

A graph of the calculated and measured pressure needed to start a bubble vs. hole diameter is shown in Figure 16.

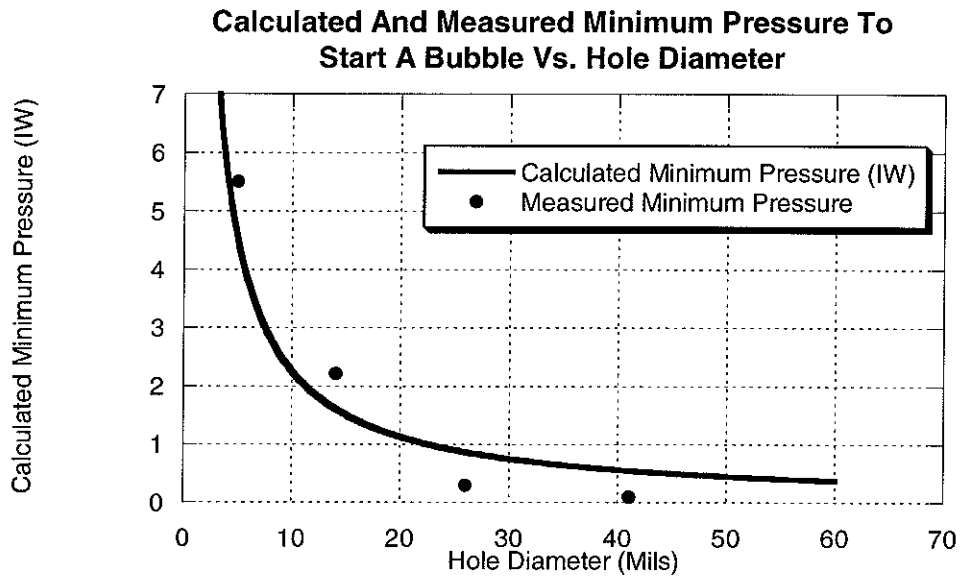


Figure 16

At a nominal pressure of 2.1 IW recommended for the pressure test, the smallest hole diameter that a bubble will form is approximately 15 mil, which is large by definition. A dangerously large inflation pressure of 25 IW would be needed to detect a 1 mil hole.

The bubble test has the advantage of actually locating the hole, not just indicating there is one. It is messy and not totally effective even for larger holes -- A bubble may burst soon after it starts and go undetected. For regions of a liner that are damaged the bubble test may be useful in determining if the defect is truly a hole. It should be noted that once a bubble has started over a hole, a much lower pressure can cause the bubble to expand.

3.4 RARE GAS TEST

The rare gas test is performed by adding a small amount of CO₂ or He to an inflated liner. A Model 21-250 GOW-MAC Gas Leak Detector was used in evaluating this method. According to the manufacture's specifications a leak rate of 1.0×10^{-5} cc/s of He or 1.1×10^{-4} cc/s of CO₂ will produce a 10% deflection of full scale.

The voltage across the analog meter of the GOW-MAC was connected to a DATAQ DI-700 A/D converter and recorded. The liner was pressurized to 1.5 IW with air, the He was added to bring the pressure to 2 IW. This corresponds to approximately 0.05 m³ of He at atmospheric pressure, or 0.13 % of the volume of the inflated liner.

The GOW-MAC probe was first slowly moved over a known hole of area approximately 1mm². The probe was then moved slowly over approximately 3 m of the upper side seam – This is the region where the translucent areas along the seam were found with the light test. A graph of the output of the GOW-MAC is shown in Figure 17. Note the much higher amplitude of the first peak as the detector was moved across the known hole.

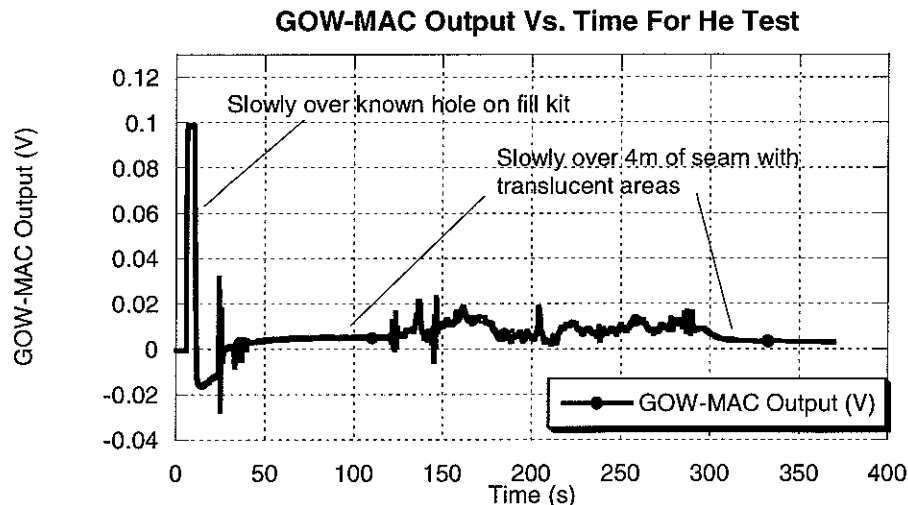


Figure 17

Conclusion

The four tests developed provide a means for reasonable quality assurance for the liners to be used in the Pierre Auger Project. Unfortunately, none of the tests as described in this paper provide a quick way to detect what we define as small holes in the liners. We can, using the tests as described, verify there are no large holes in the liners.

Since the liner has to be inflated to perform any of the discussed tests, the light test is by far the quickest way to locate holes in the liner. It is estimated that holes as small as 3.5 mil can be found quickly with the light test. The primary disadvantage of the light test is that it may not reveal some defects under a seam, which is one of the most likely locations of liner defects.

The pressure test is only sensitive to a hole size greater than 3 mm^2 , but can detect holes anywhere on the liner. Limited equipment is required because the relationship between cumulative hole size and depressurization rate has been established. A simple pressure gauge could provide the beginning and ending pressures over some length of time. Although it does lack the ability to locate holes, it is a good compliment to the light test.

The rare gas test can detect small holes similar to those found with the light test. Its primary disadvantage is it is very time consuming. The rare gas test would be useful to find holes around seams or to check liner patches.

Since we are limited to a maximum pressure of 2.1 IW the bubble test can only detect holes greater than about 15 mil. The bubble test is very time consuming when compared to the pressure and light tests. It is less sensitive than the rare gas test, but could be used around seams and patches at the factory.

List Of References

- 1 THE HIGHEST ENERGY COSMIC RAYS AND PARTICLE PHYSICS.
By G. Burdman, F. Halzen (Wisconsin U., Madison), R. Gandhi
(Harish-Chandra Res. Inst.). MADPH-97-1014, Sep 1997. 15pp.
Published in Phys.Lett.B417:107-113,1998
e-Print Archive: hep-ph/9709399

- 2 ON THE ORIGIN OF HIGHEST ENERGY COSMIC RAYS.
By G. Sigl, D.N. Schramm (Chicago U., Astron. Astrophys. Ctr. & Chicago
U., EFI & Fermilab), P. Bhattacharjee (Bangalore, Indian Inst. Astrophys.).
FERMILAB-PUB-94-080-A,
(Received Mar 1994). 21pp.
Published in Astropart.Phys.2:401-414,1994
e-Print Archive: astro-ph/9403039

- 3 http://cygnus.uchicago.edu/~blanca/app_results/node5.html

- 4 http://www.srl.caltech.edu/personnel/dick/cos_encyc.html

- 5 <http://www-hep.phys.unm.edu/auger.html>

- 6 ON THE DETECTION OF ULTRAHIGH-ENERGY NEUTRINOS WITH
THE AUGER OBSERVATORY.
By K.S. Capelle, J.W. Cronin (Chicago U., EFI), G. Parente,
E. Zas (Santiago de Compostela U.). Jan 1998. 15pp.
Published in Astropart.Phys.8:321-328,1998
e-Print Archive: astro-ph/9801313

- 7 NEUTRINO INDUCED GIANT AIR SHOWERS IN LARGE EXTRA
DIMENSION MODELS.
By Ambar Jain, Pankaj Jain (Indian Inst. Tech., Kanpur), Douglas W. McKay,
John P. Ralston (Kansas U.). Nov 2000. 21pp.
e-Print Archive: hep-ph/0011310

- 8 NEUTRINO INDUCED EVENTS IN THE PIERRE AUGER DETECTOR.
By Gonzalo Parente, Enrique Zas (Santiago de Compostela U.).
US-FT-28-96, Feb 1996. 9pp.
Presented at 7th International Workshop on Neutrino Telescopes,
Venice, Italy, 27 Feb - 1 Mar 1996.
e-Print Archive: astro-ph/9606091

- 9 <http://www.physics.adelaide.edu.au/astrophysics/high.html>

- 10 <http://www.sciam.com/specialissues/0398cosmos/0398croninbox1.html>
- 11 P. Auger et al., Comptes Rendus 206 (1938) 1721.
- 12 AUGER PROJECT SEEKS TO STUDY HIGHEST ENERGY COSMIC RAYS.
By B. Schwarzschild. 1997.
Published in Phys.Today 50N2:19-21,1997
- 13 THE PIERRE AUGER OBSERVATORY.
By AUGER Collaboration (D. Zavrtanik for the collaboration). 2000.
Published in Nucl.Phys.Proc.Suppl.85:324-331,2000
- 14 THE PIERRE AUGER PROJECT: AN OBSERVATORY FOR THE HIGHEST ENERGY COSMIC RAYS.
By C.K. Guerard (INFN, Milan). 1999.
Given at 10th International Symposium on Very High-Energy Cosmic Ray Interactions (ISVHECRI 98), Assergi, Italy, 12-17 Jul 1998.
Published in Nucl.Phys.Proc.Suppl.75A:380-382,1999
- 15 EXTREMELY HIGH-ENERGY COSMIC RAYS AND THE AUGER OBSERVATORY.
By Murat Boratav (Paris U., VI-VII). May 1996. 13pp.
Talk given at 7th International Workshop on Neutrino Telescopes, Venice, Italy, 27 Feb - 1 Mar 1996.
Published in Nucl.Phys.Proc.Suppl.48:488-490,1996
e-Print Archive: astro-ph/9605087
- 16 COSMIC RAYS AT THE ENERGY FRONTIER.
By J.W. Cronin, S.P. Swordy (Chicago U., Astron. Astrophys. Ctr.), T.K. Gaisser (Delaware U.). 1997.
Published in Sci.Am.276:32-37,1997 (No.1) (Issue no.1)
- 17 PERFORMANCE OF THE CERENKOV COUNTERS IN THE FERMILAB TAGGED PHOTON SPECTROMETER FACILITY.
By David Bartlett, Sampa Bhadra, Lucien Cremaldi, Alan Duncan, Don Edmonds, James Elliott, Mark Gibney, Uriel Nauenberg, Gerhard Schultz (Colorado U.), Gerd Hartner (Toronto U.). COLO-HEP-121, Nov 1986. 66pp.
Published in Nucl.Instrum.Meth.A260:55,1987 . Bartlett's Cherenkov detector was used in the Fermilab charm hadroproduction experiment E791 which is described in E. M. Aitala et al., EPJdirect C4 (1999) 1 and S. Bracker et al., IEEE Trans. Nucl. Sci. 43 (1996) 2457.

- 18 RESULTS AND CURRENT STATUS OF THE WATER CERENKOV DETECTOR DEVELOPMENT FOR THE AUGER SURFACE ARRAY. By T. Kutter (Chicago U., Astron. Astrophys. Ctr.). 1999. Given at 10th International Symposium on Very High-Energy Cosmic Ray Interactions (ISVHECRI 98), Assergi, Italy, 12-17 Jul 1998. Published in Nucl.Phys.Proc.Suppl.75A:383-385,1999
- 19 <http://www.he-astro.physics.utah.edu/Auger.html>
- 20 <http://www.ras.ualgary.ca/SKA/science/node11.html>
- 21 UPPER LIMIT OF THE SPECTRUM OF COSMIC RAYS. By G.T. Zatsepin, V.A. Kuzmin (Lebedev Inst.). Aug 1966. Published in JETP Lett.4:78-80,1966, Pisma Zh.Eksp.Teor.Fiz.4:114-117,1966.
- INFLUENCE OF THE UNIVERSAL MICROWAVE BACKGROUND RADIATION ON THE EXTRAGALACTIC COSMIC RAY SPECTRUM. By F.A. Aharonian (Heidelberg, Max Planck Inst.), J.W. Cronin (Fermilab & Chicago U., EFI). 1994. Published in Phys.Rev.D50:1892-1900,1994
- 22 ULTRA HIGH ENERGY COSMIC RAYS. By J.W. Cronin (Chicago U., Astron. Astrophys. Ctr.). 2001. Published in Nucl.Phys.Proc.Suppl.97:3-9,2001 Also in "Campinas 2000, Very high energy cosmic ray interactions"
- 23 COSMIC RAYS: THE MOST ENERGETIC PARTICLES IN THE UNIVERSE. By J.W. Cronin (Chicago U., Astron. Astrophys. Ctr.). 1999. Published in Rev.Mod.Phys.71:S165-S172,1999
- 24 <http://www.ses-ng.si/public/pao/paop.html>
- 25 COSMIC TOPOLOGICAL DEFECTS, HIGHEST ENERGY COSMIC RAYS, AND THE BARYON ASYMMETRY OF THE UNIVERSE. By Pijushpani Bhattacharjee (NASA, Goddard & Bangalore, Indian Inst. Astrophys.). Mar 1998. 4pp. Published in Phys.Rev.Lett.81:260-263,1998 e-Print Archive: hep-ph/9803223

- 26 RELIC NEUTRINOS AND Z RESONANCE MECHANISM FOR HIGHEST ENERGY COSMIC RAYS.
By James L. Crooks, James O. Dunn, Paul H. Frampton (North Carolina U.).
IFP-778-UNC-A, Feb 2000. 11pp.
Published in *Astrophys.J.*546:L1-L4,2001
e-Print Archive: astro-ph/0002089
- 27 STRONGLY INTERACTING NEUTRINOS AND THE HIGHEST ENERGY COSMIC RAYS.
By G. Domokos, S. Kovesi-Domokos (Johns Hopkins U.).
JHU-TIPAC-98013, Dec 1998. 9pp.
Published in *Phys.Rev.Lett.*82:1366-1369,1999
e-Print Archive: hep-ph/9812260
- 28 Cremaldi, Holcomb, Booke. Bag Liner Quality Control-I (GAP 2000-057)

Appendix A

Calculating Leak Rates For Pressure Test

The following calculations relate the leak rate to the effective area of hole in the liner.

ρ Current density of air. m_{Air} Mass of one air particle

ρ_0 Density of air at STP T Temperature

P Absolute Pressure T_0 273.13K

P_A Atmospheric Pressure a Effective area of hole

V Volume of liner

$$\rho \equiv \frac{\rho_0 P T_0}{P_A T}$$

$$PV = nk_B T$$

$$\Delta P = \frac{\Delta n k_B T}{V}$$

$$\Delta P m_{Air} = \frac{\Delta m k_B T}{V}$$

$$\Delta m = v a \rho \Delta t = a \sqrt{\frac{2\Delta P}{P T_0}} \rho_0 \frac{P T_0}{P_A T} \Delta t = a \sqrt{\frac{2\Delta P P \rho_0 T_0}{P_A T}} \Delta t$$

$$\frac{\Delta P}{\Delta t} = \frac{a}{m_{Air} V} \sqrt{\frac{2\Delta P P \rho_0 T_0}{P_A T}} k_B T = \frac{a k_B}{m_{Air} V} \sqrt{\frac{2\Delta P P \rho_0 T_0 T}{P_A}}$$

$$A = \frac{a k_B}{m_{Air} V} \sqrt{\frac{2\rho_0 T_0 T}{P_A}} = 10.9 a \frac{1}{s} \text{ Assuming a } 38\text{m}^3 \text{ volume.}$$

$$\frac{dP}{dt} = -A \sqrt{P^2 - P P_A}$$

$$\int_0^t dt = \int_{P_2}^{P_1} \frac{dP}{A\sqrt{P^2 - PP_A}}$$

$$t = \frac{1}{A} \left(2 \operatorname{Ln}(\sqrt{P} + \sqrt{P - P_A}) \right) \Big|_{P_2}^{P_1} = \frac{2}{A} \operatorname{Ln} \left(\frac{\sqrt{P_1} + \sqrt{P_1 - P_A}}{\sqrt{P_2} + \sqrt{P_2 - P_A}} \right)$$

Plugging in pressures of 1-inch and 1.5-inch gives an expression for the size of hole for a given deflation time.

$$A = \frac{.0225}{t} \text{ where } t \text{ is in seconds.}$$

P(t) is derived below:

$$\frac{dP}{dt} = -A\sqrt{P^2 - PP_A}$$

Expanding in a series about P_A

$$\frac{dP}{dt} = -A\sqrt{P_A}\sqrt{P - P_A} - \frac{A(P - P_A)^{\frac{3}{2}}}{2\sqrt{P_A}} + \frac{A(P - P_A)^{\frac{5}{2}}}{8P_A^{\frac{3}{2}}} - \dots$$

By taking the first term there is a worst-case error of 0.18% over the region interest.

Letting $k = A\sqrt{P_A}$ and solving $\frac{dP}{dt} = -A\sqrt{P_A}\sqrt{P - P_A}$ gives

$$P(t) = \frac{1}{4} (4P_A + k^2 t^2 - 2k^2 t C + k^2 C^2)$$

Solving for C when $t=0$ and $P(t) = P_0$

$$C = \frac{2}{A} \sqrt{\frac{P_0 - P_A}{P_A}}$$

Plugging in and rearranging

$$P(t) = P_0 - A t \sqrt{P_A} \Delta P_0 + \frac{1}{4} A^2 P_A t^2$$

Appendix B

Pressure Test Instrumentation

A PX139-.3D4V differential pressure transducer from Omega is used to measure the pressure in the liner. The transducer has a compensated temperature range from 0⁰C to 50⁰C, and a maximum error of 0.5% due to non-linearity and hysteresis. It requires a 5V supply and the output of the transducer is approximately 2.500 V when both pressure inputs are open to the atmosphere.

The output of the transducer is $\pm 2V$ from zero pressure differential over a range of ± 0.3 PSI, or ± 8 IW. The range of pressures used in the inflation test are 0 IW to +2.5 IW, which correspond to a maximum ΔV of 600mV. A DIY Kit 93 PC Data Acquisition Unit is used to monitor the output of the pressure transducer. The 10-bit A/D converter has a 5V range, so each channel is approximately 5mV.

The output of the transducer is amplified to maximize to resolution of the pressure readings. Gain was selected such that the output of the amplifier would be 2V per 1 IW.

$$G\left(0.2474 \frac{V}{inch}\right) = 2.0 \frac{V}{inch} \Rightarrow G = 8.084 \quad (B.1)$$

Where G is the desired gain. An AD620AN IA (Instrument Amplifier) is used to amplify the output of the pressure transducer. Figure B.1 shows a schematic of the amplifier circuit.

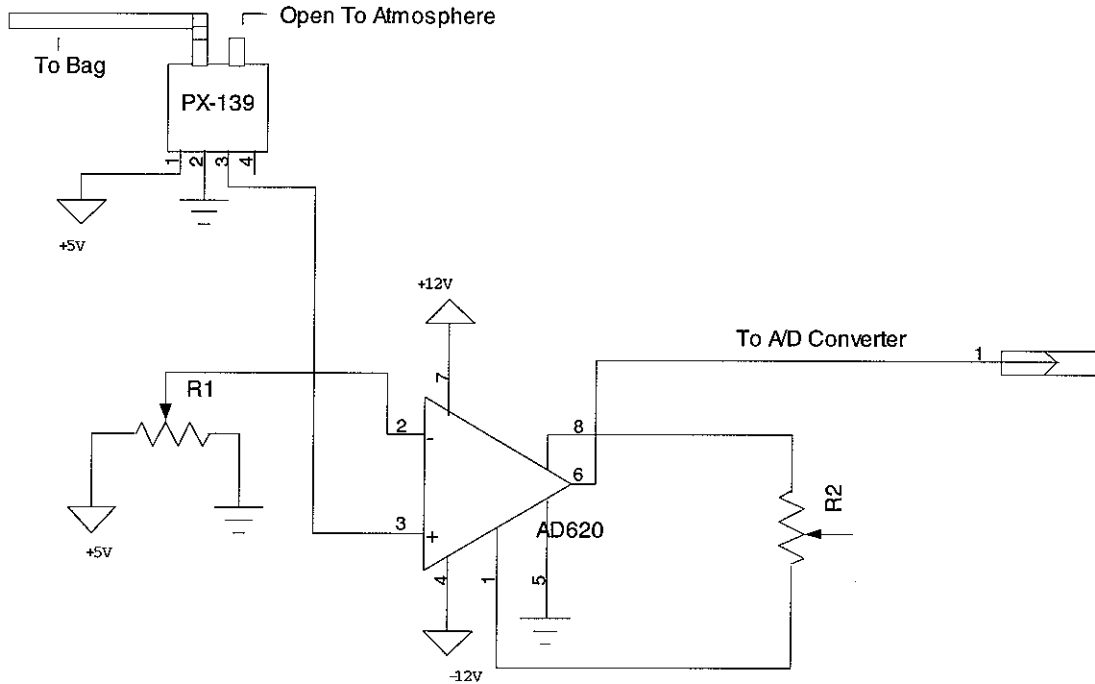


Figure B.1

The output of the pressure transducer is approximately 2.50 V when both pressure inputs are open to the atmosphere. R1 is used as a voltage divider and fed into the inverting input of the IA. Adjusting R1 allows zeroing of the output for zero pressure differential.

From the data sheet of the IA the resistor used to set the gain is:

$$R_G = \frac{49.4K\Omega}{G - 1} = 6.97K\Omega \quad (\text{B.2})$$

Where R_G is the gain resistor

R_G is a 10-turn 10K Ω potentiometer that allows the resistance to be reliably set to the required accuracy. R_G becomes the second element in a voltage divider with a 49.4K Ω

resistor inside the IA. Since both are carbon, and have the same temperature coefficient, temperature effect on gain is minimal.

To verify the gain and linearity of the amplifier a test circuit was constructed, and the following data in Table B.1 was taken. Instead of using the pressure transducer, a 10-turn 1K Ω potentiometer was used to provide the differential voltage

Absolute (V)	Relative (V)	Output (V)
2.600	0.100	0.796
2.700	0.200	1.613
2.802	0.302	2.434
2.899	0.399	3.216
2.999	0.499	4.026
3.101	0.601	4.852

Table B.1

A linear curve fit gives a slope, or gain, of 8.087. This is under 0.04% of the designed gain. A plot of the curve fit and data is shown below in Figure B.2.

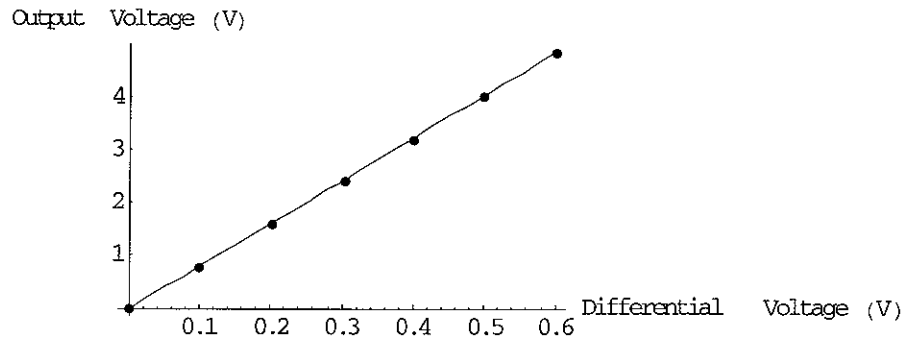


Figure B.2

As an additional test, a Dwyer Magnehelic, 4 IW full scale, and the circuit were attached to the liner at various pressures. The constructed circuit's readings were consistent with those of the Magnehelic.

A MS-DOS program was written to interface with the A/D converter. The program writes the data to disk, and also displays a scrolling window of time and pressure data. The A/D channel used, output file, length of experiment, and sample interval can be set by editing the configuration file. The C listing is in appendix C.

As a test of stability a simulated (constant) pressure differential was connected to the circuit. The plot and histogram for a two-hour pedestal taking readings every 10 seconds is shown in Figures B.3 and B.4. The R.M.S. deviation is 0.0022 IW.

Pressure vs. Time With Zero Pressure Differential And Added Offset

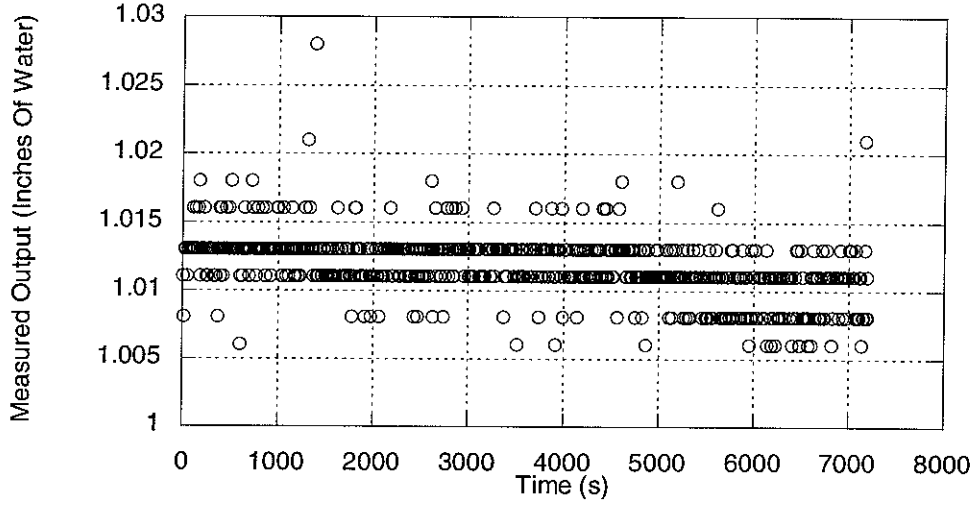


Figure B.3

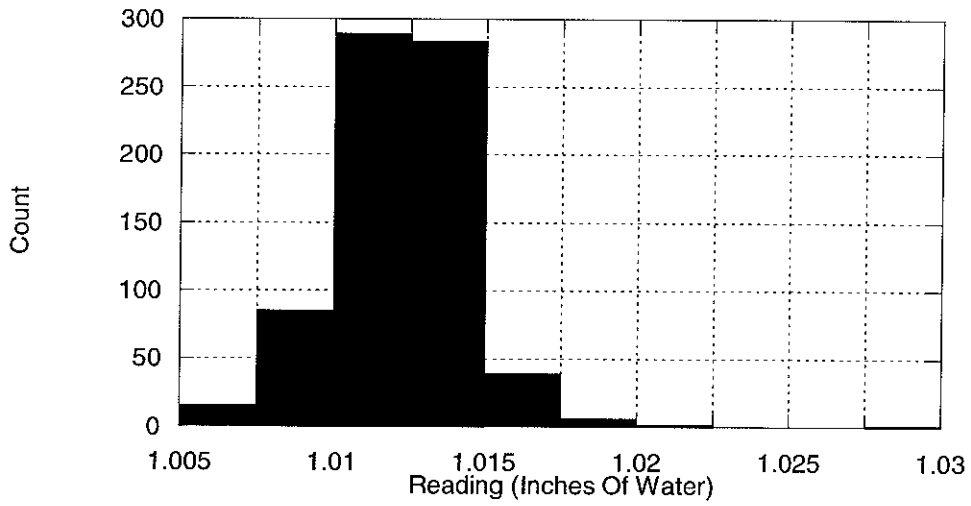


Figure B.4

Appendix C

This is the MS-DOS C program written to acquire pressure data from the A/D converter.

This file calls a function ReadData() (Not Listed Here), that came with the A/D converter.

```
#include <stdio.h>
#include <stdlib.h>
#include <string.h>
#include <time.h>
#include <conio.h>
#include <ctype.h>
#include <dos.h>

#define _ulc 201
#define _urc 187
#define _llc 200
#define _lrc 188
#define _hz 205
#define _vert 186

void DrawBox(int x, int y, int width, int height);
void ScrollBox(void);
int fpfloatemp( const void *a, const void *b);
void ReadConfig(char *cfn = NULL);

extern "C" int ReadData(int channel,int *chn, float *dta);

int channel, chntoread=9;
long interval=10, runlength=240;
char coutfile[80];
float freadings[5];
float ftemp, fatm;
void main(void)
{
    int i;
    int CurY;
    FILE *out;
    time_t starttime, elapsedtime=0;
    strcpy(coutfile, "newdat.txt");

    clrscr();
    fflush(stdin);

    /* Read in bagtest.cfg for test parameters*/
    ReadConfig();

    if ((out = fopen(coutfile, "wt")) == NULL)
    {
        printf("Could not create output file");
    }
}
```

```

        exit(-1);
    }

    /* Display output filename, interval and duration */
    gotoxy(5,2);
    printf("Reading channel : %d",chntoread);
    gotoxy(5,3);
    printf("Reading every : %ld seconds for %ld minutes",interval,runtime);
    gotoxy(5,4);
    printf("Writing to %s",outfile);
    gotoxy(31,24);
    printf("Press any key to end");

    /* Draw box on screen and set up scrolling */
    DrawBox(7,5,60,15);
    CurY = 7;

    /* Begin taking data for runtime minutes, or a key is pressed */

    starttime = time(NULL);

    while(1)
    {
        elapsedtime = time(NULL) - starttime;
        for(i=0;i<5;i++) ReadData(chntoread,&channel,&freadings[i]);

        /* Sort the five readings */
        qsort(freadings,5,sizeof(float),fpfloatcmp);

        /* get temp reading */
        ReadData(7,&channel,&ftemp);
        ftemp *= 100;
        ReadData(5,&channel,&fatm);
        fatm -= .5;
        fatm /= .266667;
        if(CurY < 18) CurY++;
        else ScrollBox();

        gotoxy(15,CurY);
        printf("%-7ld\t",elapsedtime);
        fprintf(out,"%ld\t",elapsedtime);

        /* Report the median reading */

        printf("%-8.3f  %-4.2f  %-4.2f",freadings[2]/2,fatm,ftemp);
        fprintf(out,"%-8.3f  %-4.2f  %-4.2f\n",freadings[2]/2,fatm,ftemp);

        while(elapsedtime + interval > time(NULL) - starttime)
        {
            if(kbhit() || elapsedtime > runtime * 60)
            {
                fclose(out);
                clrscr();
                exit(0);
            }
        }
    }

```

```

        } /* delay while */

    } /* while */
} /* main */

void DrawBox(int x, int y, int width, int height)
{
    int i,ofs=(width)*2;
    char far *scrptr;
    char far *Base =(char*) MK_FP(0xb800,x*2+y*160);
    gotoxy(15,5);
    printf("time(s)");
    gotoxy(23,5);
    printf("inches  atm(lbs)  temp (C)");

    *(Base) = _ulc;
    *(Base + width * 2) = _urc;
    *(Base + height * 160) = _llc;
    *(Base + height * 160 + width *2) = _lrc;
    scrptr = Base + 2;

    for(i=0;i<width-1;i++,scrptr+=2) *scrptr = _hz;
    scrptr = Base + height*160 +2;
    for(i=0;i<width-1;i++,scrptr+=2) *scrptr = _hz;
    scrptr = Base + 160;
    for(i=1;i<height;i++)
    {
        *scrptr = _vert;
        scrptr += ofs;
        *scrptr = _vert;
        scrptr += 160 - ofs;
    }
}

void ScrollBox(void)
{
    union REGS regs;
    regs.h.ah = 6; /* set cursor position */
    regs.h.al = 1;
    regs.h.bh = 7; /*white on black*/
    regs.h.ch = 7;
    regs.h.cl = 12;
    regs.h.dh = 18;
    regs.h.dl = 65;
    int86(0x10, &regs, &regs);
}

/* Used for qsort */

int fpfloatcmp( const void *a, const void *b)
{
    if(*(float*)a==*(float*)b) return 0;
    return (*(float*)a<*(float*)b) ? -1:1;
}

```

```
/* Called at startup to set parameters. If the file, or data in the
file is missing, a set of default parameters are used */
```

```
void ReadConfig(char *cfn)
{
    FILE *in,*out;
    char cdatfile[80];
    char *strptr;
    char instr[120];
    /* set the default values if some or all settings are
missing from config file */
    interval = 10;
    runlength = 240;
    chntoread= 9;

    if(!cfn) strcpy(cdatfile,"bagtest.cfg");
    else strcpy(cdatfile,cfn);

    if ((in = fopen(cdatfile, "rt"))== NULL)
    {
        printf("\nCannot open config file. Use default values? (Y|N) ");
        if(toupper(getche()) != 'Y') exit(1);
        clrscr();
        return;
    }

    while(fgets(instr,80,in))
    {
        strupr(instr);
        strptr = instr;
        switch(instr[0])
        {

            case 'C':
                if(strcmp(instr,"CHANNEL="))
                {
                    strptr += strlen("CHANNEL=");
                    if(isdigit(*strptr))
                    {
                        if((chntoread = atoi(strptr)) > 9) chntoread = 9;
                    }
                }
                break;

            case 'I':
                if(strcmp(instr,"INTERVAL="))
                {
                    strptr += strlen("INTERVAL=");
                    if(!isdigit(*strptr)) break;
                    interval = atoi(strptr);
                    if(!interval) interval = 10;
                }
                break;

            case 'D':
```



```

if(strcmp(instr,"DURATION="))
{
    strptr += strlen("DURATION=");
    if(!isdigit(*strptr)) break;
    runlength = atoi(strptr);
    if(!runlength) runlength = 240;
}
break;

case 'O' :
if(strcmp(instr,"OUTPUT="))
{
    strptr += strlen("OUTPUT=");
    strptr[strlen(strptr+1)] =0;
    strcpy(coutfile,strptr);
    /* open/create to see if valid filename */
    if ((out = fopen(coutfile,"wt")) == NULL)
    {
        strcpy(coutfile,"bagtest.cfg");
    }
    else fclose(out);
}
break;
        } /* switch */
    } /* while */
} /* ReadConfig */

```